Excitation Function and Integral Recoil Properties of the $Cu^{65}(p,p\pi^+)Ni^{65}$ Reaction*

L. P. REMSBERG
Chemistry Department, Brookhaven National Laboratory, Upton, New York
(Received 2 December 1964)

The excitation function for the $Cu^{65}(p,p\pi^+)Ni^{65}$ reaction was measured from 0.49 to 28 GeV. With other data, this provides a complete excitation function for this reaction from threshold to 28 GeV. The excitation function is dominated by a broad peak at ~1.3 GeV which is due to the $(\frac{3}{2},\frac{3}{2})$ π^+-p resonance. Thick-target, integral recoil experiments were performed at 2.8 and 28 GeV. The experimental excitation function and the results of the recoil experiments were compared with the results of an improved version of the calculation of Ericson, Selleri, and Van de Walle. Agreement between the experimental data and the calculations is obtained only when the one-pion-exchange (OPE) theory is used to describe the inelastic p-p interaction occurring in the nucleus. These results indicate that the treatment of the $(p,p\pi^+)$ reaction by Ericson *et al.* is basically correct and that OPE theory remains valid at energies up to 28 GeV, at least at the low momentum transfers selected by the $(p,p\pi^+)$ reaction. These data also suggest that the exchange of one unit of isotopic spin at very high energies is not greatly suppressed at low momentum transfers.

I. INTRODUCTION

RECENTLY, Ericson, Selleri, and Van de Walle[1] have pointed out that certain simple high-energy spallation reactions, such as the $(p,p\pi^+)$ reaction, should select events which take place only at low momentum transfer in the interaction between the incident particle and a nucleon in the nucleus. The elementary particle reaction which occurs in the nucleus in a $(p,p\pi^+)$ reaction is

$$p+[p]\rightarrow[n]+p+\pi^+, \quad (1)$$

where the brackets indicate that the target proton is bound in the target nucleus and the recoil neutron is bound in the product nucleus. More than one pion may be produced provided that the net charge of all the pions is $+1$.[2] The excitation energy of the residual nucleus must be less than the effective threshold for particle emission or the $(p,p\pi^+)$ reaction product will not be observed. This in turn imposes the restriction that the momentum transfer must be less than about twice the Fermi momentum. Thus the nucleus can be considered as a detector for reaction (1) at momentum transfers less than ~0.5 GeV/c.

Much of the interest in the $(p,p\pi^+)$ reaction arises from this selection of low momentum transfers in the elementary particle reaction occurring within the nucleus. It is just at these momentum transfers that the "simple" one-pion-exchange (OPE) theory (i.e., in the pole approximation) has been successful in accounting for the experimental data on single pion production in proton-proton collisions at incident energies from 1 to 3 GeV.[3–5] Ferrari and Selleri[3,4] have extended the validity of OPE theory to all momentum transfers by including a correction for the effects of off-the-mass-shell pion-proton scattering and introducing a correction which they ascribe to the pionic form factor. These corrections, however, are relatively small throughout most of the range of momentum transfers sampled by the $(p,p\pi^+)$ reaction.

Ericson *et al.*[1] presented a simple calculation of the $(p,p\pi^+)$ excitation function. They used OPE theory in the pole approximation to describe the elementary particle reaction and a degenerate Fermi gas model of the nucleus for the evaluation of the nuclear form factors. The purpose of the present work was to test the validity of the treatment of Ericson *et al.* and also to attempt to use the $(p,p\pi^+)$ reaction to obtain some information bearing on the applicability of OPE theory at 28 GeV.

The excitation function of the $Cu^{65}(p,p\pi^+)Ni^{65}$ reaction was measured from 0.49 to 28 GeV. With previous data[6–9] this provides a complete excitation function for this reaction from threshold to 28 GeV for comparison with the calculation. Thick-target, integral recoil ranges were measured at incident energies of 2.8 and 28 GeV to obtain average values of the projections of the kinetic energies of the recoiling nuclei both parallel and perpendicular to the beam direction. Conversion of the forward effective recoil range to the average of the projections of the recoil energies along the beam direction is possible only because recoils in the backward direction are kinematically forbidden for the $(p,p\pi^+)$ reaction. These recoil measurements are of interest because the momentum of the recoiling product nucleus from a $(p,p\pi^+)$ reaction is essentially identical

* Research performed under the auspices of the U. S. Atomic Energy Commission.

[1] T. Ericson, F. Selleri, and R. T. Van de Walle, Nucl. Phys. **36**, 353 (1962).

[2] Unless otherwise indicated, reaction (1) will always be taken to include all reactions involving multiple pion production and even strange particle production provided only that there is a recoil neutron.

[3] E. Ferrari and F. Selleri, Nuovo Cimento, Suppl. **24**, 453 (1962).

[4] E. Ferrari and F. Selleri, Nuovo Cimento **27**, 1450 (1963).

[5] D. V. Bugg, A. J. Oxley, J. A. Zoll, J. G. Rushbrooke, V. E. Barnes, J. B. Kinson, W. P. Dodd, G. A. Doran, and L. Riddiford, Phys. Rev. **133**, B1017 (1964). See Ref. 3 for a comprehensive list of references on comparisons between OPE theory and experimental results.

[6] S.-C. Fung and A. Turkevich, Phys. Rev. **95**, 176 (1954).

[7] V. P. Crespo, Rev. Port. Quim. **5**, 6 (1963).

[8] D. W. Barr, University of California, Lawrence Radiation Laboratory Report No. UCRL-3793 (unpublished) and private communication.

[9] G. Rudstam, Nucl. Phys. **56**, 593 (1964).

with the momentum transfer in the elementary-particle reaction (1) taking place within the nucleus. Thus the nucleus in a $(p,p\pi^+)$ reaction can be thought of not only as a detector for reaction (1) at low momentum transfer but also as a detector for the recoil neutron in reaction (1), capable of measuring both the angle and magnitude of the momentum transfer.

In this paper the calculation of Ericson *et al.*[1] has been extended to include calculations of the averages of the projected recoil energies for comparison with the measured values. The calculation has been improved to the extent of eliminating some of the approximations employed by Ericson *et al.* in their evaluation of the nuclear form factors, although the Fermi gas model of the nucleus has been retained.

The experiments are described in Sec. II, and the results are analyzed in Sec. III, comprising mostly the evaluation of the contributions from the secondary (n,p) reaction and the conversion of recoil ranges to energies. The calculation is presented and compared with the experimental results in Sec. IV, and Sec. V consists of conclusions.

II. EXPERIMENTAL

The cross sections obtained in these experiments were all measured relative to the cross section for the $Al^{27}(p,3pn)Na^{24}$ reaction. The cross sections for the production of both Ni^{65} and Ni^{57} for proton energies less than 2.8 GeV were measured directly relative to the monitor reaction. At 2.8 and 28 GeV, however, the Ni^{57} cross sections were obtained from monitored targets while the Ni^{65} cross sections were generally obtained from $\sigma(Ni^{65})/\sigma(Ni^{57})$ ratios from unmonitored targets. This procedure was followed for two reasons. The recoil targets were not monitored but yielded $\sigma(Ni^{65})/\sigma(Ni^{57})$ ratios. The contributions of the secondary (n,p) reaction were measured at these two energies by measuring the Ni^{65} cross section as a function of target thickness. Since the $\sigma(Ni^{65})/\sigma(Ni^{57})$ ratio can be determined much more accurately than either cross section, the use of the ratio results in a more precise extrapolation to zero target thickness. The contribution of secondaries to the Ni^{57} cross sections is negligible at the target thicknesses used in these experiments. Also, the absence of the monitor foil results in thinner targets and reduces the extrapolation.

All targets were irradiated in the internal proton beams of the Brookhaven Cosmotron or AGS. Three types of targets were used. The targets for which the beam intensity was monitored consisted of a Cu target foil, a 0.001-in. Al monitor foil, and two or three Al guard foils. The foils for the Cosmotron targets were aligned with shears prior to irradiation except for one guard foil which protruded 0.5–1 mm beyond the leading edge of the aligned foils. This was intended to reduce the variation in beam intensity across the foil stack and thus reduce any errors due to possible misalignment. Alignment of the foils in the monitored AGS targets was achieved by punching a $\frac{7}{16}$-in.-diam circle through the foil stack about 1 mm back from the leading edge after the irradiation. When only the $\sigma(Ni^{65})/\sigma(Ni^{57})$ ratio was to be measured, the target consisted of a Cu foil and two Al guard foils.

The forward effective recoil range FW of a product of a given nuclear reaction is the fraction of the total activity which recoils out of the target foil in the forward direction F times the target thickness W. The backward and perpendicular effective recoil ranges BW and PW are defined similarly. The targets for the recoil measurements consisted of a Cu target foil, two 0.00025-in. Mylar catcher foils, one 0.00025-in. Mylar foil for an activation blank, and two 0.00025-in. Mylar guard foils. The Mylar foils were all cut to the same size and protruded 0.5–1 mm beyond the target foil. Prior to irradiation, both the Mylar foils and the target foil were degreased with organic solvents, and the Cu foil was cleaned in either 30% HNO_3 or 50% HCl. Etching was not allowed to take place since it was felt that a smooth shiny surface was superior to an etched surface for recoil measurements. The targets used for measuring the forward and backward effective recoil ranges were perpendicular to the beam, and those used for measuring perpendicular effective recoil ranges were oriented at an angle of 10° to the beam.

All of the Cu targets from which cross sections for the production of Ni^{65} were measured, either directly or relative to the cross section for Ni^{57}, were taken from the same stock of 0.00033-in. Cu foil whose purity was greater than 99.99%.[10] The thicker targets were made up of several layers of this foil. The contribution to the production of Ni^{65} from impurities in the Cu foils was investigated by looking for Ni^{66}. Its daughter Cu^{66} was milked from a purified Ni fraction from a Cu target irradiated with 2.8-GeV protons. No Cu^{66} activity was detected, and conditions of the experiment established an upper limit for the production of Ni^{66} of 0.1 μb. Since the cross sections for producing Ni^{65} from various targets with high-energy protons range from 2–10 times larger than the cross sections for producing[11] Ni^{66}, it can be concluded that the impurities contribute less than 1 μb to the production of Ni^{65} in the Cu foil used.

The energies of the protons during the 0.49- and 0.65-GeV runs were calculated from measurements of the revolution frequency and radius of the circulating proton beam at the time acceleration was stopped and are accurate to about 15 MeV. The energies for the other runs were obtained from magnetic field measurements supplied by the operating staffs of the Cosmotron and AGS and are accurate to about 5%.

After the irradiations the target foils were dissolved in dilute HNO_3, and the Mylar catcher foils were dissolved and wet ashed in a mixture of two parts $HClO_4$

[10] Spectrographic analysis kindly performed by M. Slavin.

[11] E. Bruninx, European Organization for Nuclear Research Reports No. CERN 61-1, 1961, and CERN 62-0, 1962 (unpublished).

TABLE I. Results of the individual experiments for cross sections only.

T (GeV)	Target composition (mg/cm²)	$\sigma(Ni^{65})$[a] (mb)	$\sigma(Ni^{57})$[a] (mb)
0.49	7.4 Cu, 12.1 Al	0.142	1.30
0.65	7.4 Cu, 12.1 Al	0.209	1.13
1.0	7.4 Cu, 12.1 Al	0.234	0.821
1.4	7.4 Cu, 12.1 Al	0.240	0.729
2.0	7.4 Cu, 12.1 Al	0.213	0.655
2.8	7.4 Cu, 4.3 Mylar	0.171[b]	...
2.8	45.4 Cu, 14.5 Al	...	0.617
2.8	59.2 Cu, 14.5 Al	0.204[b]	0.570
28	7.4 Cu, 4.3 Mylar	0.102[b]	...
28	22.2 Cu, 5.2 Al	0.113[b]	...
28	44.3 Cu, 5.2 Al	0.125[b]	...
28	73.8 Cu, 5.2 Al	0.140[b]	...
28	12.7 Cu, 28.5 Al	...	0.481
28	12.7 Cu, 28.5 Al	...	0.519

[a] The $\sigma(Ni^{65})$ values were calculated from the Cu^{65} content of the targets, and the $\sigma(Ni^{57})$ values were calculated from the total Cu in the targets.
[b] Computed from the measured $\sigma(Ni^{65})/\sigma(Ni^{57})$ ratio and the average Ni^{57} cross sections in Table III.

and one part HNO_3. Two milligrams of Ni carrier were present, and standard radiochemical procedures were used to isolate and purify the Ni fractions. The Ni samples were mounted for radioactivity measurements as the dimethyl glyoxime derivative, and chemical yields were later determined spectrophotometrically.

The disintegration rates of the Ni nuclides were determined with end-window, methane-flow proportional counters which had been calibrated directly for these two nuclides as a function of sample thickness. The calibration for Ni^{57} was performed with the positron annihilation coincidence method[12] with the number of positrons per decay taken to be[13] 0.47. The Ni^{65} calibration was based on standards whose disintegration rates were determined in a 4π β counter.[14] The samples for the 4π counter were prepared by vacuum evaporation of nickel dimethyl glyoxime and were 3–4 $\mu g/cm^2$ thick.[15] The disintegration rates of Na^{24} in the Al monitor foils were determined with end-window, argon-methane-flow proportional counters which had been calibrated for Na^{24} in 0.001-in. Al foil by the β-γ coincidence method. The accuracy of all of these calibrations is estimated to be 2–3%. A least-squares computer program[16] was used to resolve the Ni decay curves into 2.58-h and 36-h components.

III. RESULTS

The results of the individual runs, along with the target compositions, are listed in Tables I and II. The Ni^{65} cross sections are based on an abundance of Cu^{65} in natural Cu of 0.309.[13] The Ni^{65} cross sections at 2.8 and 28 GeV were obtained from $\sigma(Ni^{65})/\sigma(Ni^{57})$ ratios and were calculated from the corrected average Ni^{57} cross sections. All of the cross sections in Tables I and II have been corrected for recoil loss. This was measured at 2.8 and 28 GeV and the correction for Ni^{65} at the other energies was obtained from the solid curve in Fig. 4 (to be described later). Since the total recoil range, forward plus backward, for Ni^{57} at 2.8 GeV was found to be identical with that reported by Fung and Turkevich[6] at 0.41 GeV, it was used to correct all of the Ni^{57} data below 2.8 GeV.

The effective cross section for the $Cu^{65}(n,p)Ni^{65}$ reaction initiated by secondary neutrons should be proportional to the average path length of the secondary neutrons in the Cu target foil which can be estimated as a function of target geometry. We assume that the secondary neutrons are produced with an isotropic distribution from a point beam in the center of a circular target foil of radius r and thickness $t(t \ll r)$, and that there is no absorption of the neutrons in the target. One then obtains for the average path length $\bar{l}$ for secondary neutrons in the target foil

$$\bar{l}_{\rm int}=\frac{t}{2}\left(\frac{3}{2}-\ln\frac{t}{r}\right).$$

For the average path length in the target foil of neutrons originating in a foil of thickness t' and distance y from the target foil ($t' \ll r$ and $y \ll r$) we obtain

$$\bar{l}_{\rm ext}=\frac{t}{2}\left(2-\ln\frac{t+t'+y}{r}\right),$$

neglecting terms small compared with the second term inside the parentheses. We now assume that the production of secondary neutrons is proportional to mass number and obtain for the weighted average path length in the target foil of all secondary neutrons produced in the foil stack,

$$\bar{l}_{\rm tot}=\bar{l}_{\rm int}+\frac{(\rm mg/cm^2)_{ext}}{(\rm mg/cm^2)_{int}}\bar{l}_{\rm ext}.$$

One can also assume a point beam centered on the straight edge of a semicircle and simply divide the above expressions for $\bar{l}$ by 2.[17]

Since the beam distribution in these targets showed a drop off from an intense spot at the leading edge, the rectangular targets were approximated by semicircles. Good straight lines were obtained when the cross sections from Tables I and II for producing Ni^{65} were plotted against $\bar{l}$. Least-squares fits yielded an intercept at zero $\bar{l}$ of 160 μb with a slope of 7.6 μb/0.001-in. at

[12] L. P. Rembserg and J. M. Miller, Phys. Rev. **130**, 2069 (1963).
[13] *Nuclear Data Sheets*, compiled by K. Way *et al.* (Printing and Publishing Office, National Academy of Sciences–National Research Council, Washington 25, D.C., 1963).
[14] R. Withnell, Nucl. Instr. Methods **14**, 279 (1961).
[15] B. D. Pate and L. Yaffe, Can. J. Phys. **34**, 256 (1956).
[16] J. B. Cumming, in Applications of Computers to Nuclear and Radiochemistry, NAS–NS 3107, edited by G. D. O'Kelley (Office of Technical Services, Department of Commerce, Washington 25, D. C., 1963).
[17] The equation for $\bar{l}_{\rm int}$ was originally derived by A. Turkevich and the equation for $\bar{l}_{\rm ext}$ was derived by A. M. Poskanzer (private communication).

TABLE II. Results of the individual experiments for both cross sections and effective recoil ranges.

T (GeV)	Target composition (mg/cm²)	$\sigma(Ni^{65})$[a] (mb)	Ni^{65} FW (μg/cm² Cu)	Ni^{65} BW (μg/cm² Cu)	Ni^{57} FW (μg/cm² Cu)	Ni^{57} BW (μg/cm² Cu)
2.8	7.4 Cu, 4.3 Mylar	0.170	101	5.0	186	43.3
2.8	7.4 Cu, 4.3 Mylar	0.166	103	2.2	180	48.7
2.8	37.0 Cu, 11.1 Mylar	0.191	92.6	6.1	185	48.7
28	7.4 Cu, 4.3 Mylar	0.102	...	4.6	...	49.6
28	7.4 Cu, 4.3 Mylar	0.100_5	120	7.2	154	48.1
			$P_{80}W$[b]	$P_{100}W$[b]	$P_{80}W$[b]	$P_{100}W$[b]
2.8	7.2 Cu, 4.3 Mylar	0.165	55.3	42.1	116	98
2.8	7.2 Cu, 4.3 Mylar	0.175	49.4	37.6	115	93
28	7.4 Cu, 4.3 Mylar	0.100	60.6	36.2	114	90.8

[a] Computed from the measured $\sigma(Ni^{65})/\sigma(Ni^{57})$ ratio and the average Ni^{57} cross sections in Table III. The $\sigma(Ni^{65})$ values were calculated from the Cu^{65} content of the targets.
[b] $P_{80}W$ and $P_{100}W$ refer to the catcher foils on the downstream and upstream sides of the target, respectively.

2.8 GeV and an intercept of 93 μb with a slope of 8.5 μb/0.001-in. at 28 GeV.

The only information on the effective cross section for the secondary reaction at lower energies is that of Fung and Turkevich[6] who estimated a 7% contribution from the secondary (n,p) reaction at 0.41 GeV. Since it was impossible to calculate $\bar{l}$ for their targets, the assumption was made that the effective cross sections for producing Ni^{65} increase linearly with total target thickness. On this basis, slopes of 19 and 56 μb per mg/cm² were obtained at 0.41 and 2.8 GeV, respectively, and slopes for the correction of the present data below 2.8 GeV were obtained by interpolation between these two values, the slope for the secondary reaction being assumed to increase linearly with the log of the incident energy. This behavior was suggested by the increase in average deposition energy with increasing incident energy found in the Monte Carlo calculations of Metropolis *et al.*[18] The corrections never exceeded 5% and were assumed to introduce an uncertainty equal to $\frac{1}{2}$ the amount of the correction.

The corrected cross sections are listed in Table III along with the $Al^{27}(p,3pn)Na^{24}$ monitor cross sections used.[19] The standard deviations were obtained from rms combinations of 7% for the monitor cross sections, 2% for the Na^{24} counting efficiency, 3% for the counting efficiencies of each of the Ni isotopes, 1–3% for secondary corrections, and an estimated 5% for chemical yields, monitoring technique, and counter variations. The 12% uncertainty[13] in the position branching ratio for Ni^{57} was not included in the error estimates for the Ni^{57} cross sections.

TABLE III. Corrected cross sections.

T (GeV)	$\sigma(Ni^{65})$[a] (mb)	$\sigma(Ni^{57})$[a] (mb)	$\sigma(Na^{24})$ (mb)
0.49	0.137±0.012	1.30 ±0.12	10.8
0.65	0.203±0.018	1.13 ±0.10	10.8
1.0	0.227±0.020	0.821±0.074	10.5
1.4	0.231±0.020	0.729±0.066	10.0
2.0	0.203±0.018	0.655±0.059	9.5
2.8	0.160±0.014	0.594±0.053	9.2
28	0.093±0.008	0.500±0.045	8.6

[a] The $\sigma(Ni^{65})$ values were calculated from the Cu^{65} content of the targets, and the $\sigma(Ni^{57})$ values were calculated from the total Cu in the targets.

The excitation function for the $Cu^{65}(p,p\pi^+)Ni^{65}$ reaction is plotted in Fig. 1. The cross sections of Crespo[7] and Barr[8] have been normalized to the same set of $Al^{27}(p,3pn)Na^{24}$ monitor cross sections[19] used in this work and have been corrected for the secondary (n,p) reaction in the same way as the cross sections reported here. The slope for the secondary reaction at 5.7 GeV was taken to be the same as at 2.8 GeV. The cross sections of Fung and Turkevich[6] and that of Rudstam[9] were already corrected for the secondary reaction. The energies at which the cross sections of Fung and Turkevich were measured have been corrected to take into account the energy decrement due to radial oscilla-

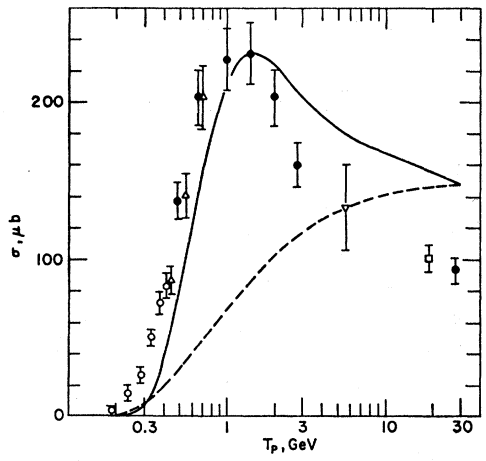

FIG. 1. Excitation function for the $Cu^{65}(p,p\pi^+)Ni^{65}$ reaction. The experimental points are: ○, Fung and Turkevich (Ref. 6); △, Crespo (Ref. 7); ▽, Barr (Ref. 8); □, Rudstam (Ref. 9); and ●, this work. The solid curve is the excitation function calculated from Eq. (7), and the dashed curve is the same calculation with a constant π^+-p total cross section replacing the experimental values.

[18] N. Metropolis, R. Bivins, M. Storm, J. M. Miller, G. Friedlander, and A. Turkevich, Phys. Rev. **110**, 204 (1958).
[19] J. B. Cumming, Ann. Rev. Nucl. Sci. **13**, 261 (1963).

TABLE IV. Corrected effective recoil ranges.

T (GeV)	Ni^{65} FW (μg/cm^2 Cu)	Ni^{65} BW (μg/cm^2 Cu)	Ni^{65} PW (μg/cm^2 Cu)	Ni^{57} FW (μg/cm^2 Cu)	Ni^{57} BW (μg/cm^2 Cu)	Ni^{57} PW (μg/cm^2 Cu)
0.41[a]	286±14	13±3	···	208±11	23 ±1	···
2.8	106± 4	2±3	48.1±3	184± 9	46.9±2	106 ±5
28	128± 6	4±3	51.2±2	154± 8	48.1±2	102.4±5

[a] Corrected data from Ref. 6.

tions in the synchrocyclotron. This correction was obtained from the work of Yule and Turkevich.[20] The agreement among the various sets of measurements is excellent. Lavrukhina *et al.*[21] have reported cross sections for the $Cu^{65}(p,p\pi^+)Ni^{65}$ reactions in the energy interval from 200 to 660 MeV. In spite of the fact that they used very thick targets (about 0.5 g/cm^2) and made no corrections for the secondary reaction, their results are in general agreement with those in Fig. 1. Because of this question of correction for the secondary reaction and also because their points show considerable scatter, they have not been included in Fig. 1.

The broad peak at $\sim$1.3 GeV in the excitation function was predicted by Ericson *et al.*[1] although it is much more pronounced and at a lower energy than in their prediction. That this peak is due to the $(\frac{3}{2},\frac{3}{2})$ pion-nucleon resonance, or first isobar, will be shown in the next section, although this is indicated qualitatively by the fact that the $(\frac{3}{2},\frac{3}{2})$ resonance occurs at an incident energy of 1.28 GeV for a proton colliding with a stationary pion.

The effective recoil ranges also must be corrected for the secondary (n,p) reaction. A recoil experiment at 2.8 GeV with a target thickness 5 times normal was performed in order to evaluate this effect. The observed recoil ranges have contributions from both the primary $(p,p\pi^+)$ and secondary (n,p) reactions according to the equation,

$$FW_t=\frac{\sigma_p}{\sigma_t}FW_p+\frac{\sigma_s}{\sigma_t}FW_s, \qquad (2)$$

where the subscripts t, p, and s refer to total, primary, and secondary, respectively. Analogous equations can be written for BW and PW. The results of the experiments at the two different target thicknesses were put into Eq. (2) yielding pairs of simultaneous equations which were solved for the primary and secondary recoil ranges. These solutions were: $FW_p=107\pm7$; $FW_s=20\pm54$; $BW_p=2.4\pm3.4$; and $BW_s=25\pm25$, all in μg/cm^2. Since the recoils from the secondary (n,p) reaction should be nearly isotropic in the lab system and essentially independent of the bombarding energy, the value for BW_s was used with Eq. (2) to correct all of the recoil ranges at both 2.8 and 28 GeV and also those measured by Fung and Turkevich[6] at 0.41 GeV. The two values of PW from each experiment were corrected for the secondary reaction, and their average was multiplied by $\pi/\cos\theta$, where θ is the angle between the target and the beam (10°), to obtain the averages of the projections of the recoils perpendicular to the beam. The $\cos\theta$ term is an approximation which would be exact only in the case of a unique recoil angle.[22] That the recoils from the $(p,p\pi^+)$ reaction approach this condition is indicated by the sidewise peaking shown by the data combined with the absence of recoils in the backward direction. No corrections were necessary for the Ni^{57} recoil data.

The corrected and averaged results of the recoil experiments are listed in Table IV. The errors for one individual determination are rms combinations of 3% for the ratio of activities in two samples, 2% for each of two chemical yields, 3% for target nonuniformity, and an error equal to the magnitude of the correction for the secondary reaction—ranging from 1 to 5% except for the BW measurements.

The kinematics of the $(p,p\pi^+)$ reaction do not allow recoils to go backward in the lab system. To show this we first reduce the problem to relativistic two-body kinematics by considering the outgoing proton and pion(s) as a single kinematic entity with a mass w which is the total energy of these outgoing particles in their own c.m. system.[23] From conservation of energy and momentum we obtain

$$q\cos\theta=(w^2-1+q^2+2E\Delta E-\Delta E^2)/2p, \qquad (3)$$

where q is the magnitude of the momentum of the recoil nucleus (the momentum transfer), E and p are the total energy and momentum, respectively, of the incident proton, and ΔE is the energy transferred to the recoil nucleus which is the excitation energy of the residual nucleus minus the Q of the reaction plus the kinetic energy of the recoil nucleus. Q is defined as the mass of the target nucleus minus the mass of the product nucleus and is usually negative. We use the units $m_p=c=1$. Since w^2 is always greater than 1.32 and since $\Delta E\ll E$ [we will henceforth drop the term ΔE^2 from Eq. (3)], $q\cos\theta$, the component of the momentum transfer parallel to the beam direction, is always positive. The small values of BW observed must therefore be due to scattering of the recoil nuclei. The maximum recoil angles obtained from Eq. (2) with the minimum w and maximum q allowed are 83° and 89° at 2.8 and 28 GeV incident energy, respectively. The value of BW observed at 0.41 GeV by Fung and Turkevich[6] would appear to have come from an extraneous source since the maximum recoil angle at this energy is 54°.

[20] H. P. Yule and A. Turkevich, Phys. Rev. **118**, 1591 (1960).
[21] A. K. Lavrukhina, I. M. Grechishcheva, and B. A. Khotin, At. Energ. (USSR) **6**, 145 (1959).
[22] J. A. Panontin, Ph.D. thesis, University of Chicago, 1962 (unpublished).
[23] We are grateful to T. Ericson for suggesting the application of two-body kinematics to the $(p,p\pi^+)$ reaction. See also A. M. Poskanzer and J. B. Cumming, Bull. Am. Phys. Soc. **8**, 325 (1963).

The range-energy curve was constructed from two sets of range measurements, both done by the thick target technique. Porile[24] measured ranges of Ga ions in Cu and Zn from (p,γ), (d,γ), and (α,γ) reactions and covered the regions from 78 to 895 keV. Bryde *et al.*[25] measured ranges of Ga ions in Cu from (α,n) reactions from 980 to 1220 keV. The heavy ion range theory of Lindhard *et al.*[26] was used to convert these ranges to ranges of Ni^{65} and Ni^{57} ions in Cu. The conversion factors averaged about 1.05 for Ni^{65} and 0.90 for Ni^{57}. Furthermore, since the range is proportional to energy, the data of Bryde *et al.* were corrected for the velocity given to the recoil ion by the evaporation of the neutron in the (α,n) reactions according to Winsberg and Alexander.[27] This correction was about 5%. There is no significant difference between the data of Bryde *et al.* and that of Porile even though the former used Au catchers and the latter used either Al or Mylar catchers. When the ranges are plotted versus energy, good straight lines with zero intercepts are obtained with slopes of 0.217 ± 0.011 μg/MeV for Ni^{65} in Cu and 0.189 ± 0.009 μg/MeV for Ni^{57} in Cu. The errors are rms combinations of 3% from the experimental data and 4% for the conversion to Ni ions in Cu. The maximum energy for the recoils from the $Cu^{65}(p,p\pi^+)Ni^{65}$ reaction is about $2\frac{1}{2}$ MeV and is probably even higher for the Ni^{57} recoils, while the range-energy data only go up to about 1 MeV. However, the theoretical work of Lindhard *et al.* indicates that the range for these ions should remain proportional to energy, within 2%, up to 3 MeV. The best straight line through the experimental range-energy data differs from the calculations of Lindhard *et al.* by only 4%.

Corrections for scattering of the recoil nuclei in the target and catcher foils have been applied to neither the recoil data in Table IV nor to the data[24,25] used to construct the range-energy curve. Such corrections, if known, would reduce the measured values of *FW*, *PW*, and *BW*. Estimates based on a simplified model of scattering indicate that the corrections on *FW* and *PW* for the $(p,p\pi^+)$ reaction are about twice as large as the corrections to the data used for the range-energy curve. Thus the scattering correction will be partially compensated through the use of the "uncorrected" range-energy curve. The calculation also indicates that the remaining, uncompensated, correction for *FW* and *PW* is less than about 5%, and furthermore that the correction should be very nearly the same for both *FW* and *PW* at both 2.8 and 28 GeV. Thus, the values of *FW* and *PW* in Table IV may be too large by as much as 5%, but neither the energy dependence of these quantities nor the *FW*/*PW* ratios are affected by the unknown scattering correction.

[24] N. T. Porile, Phys. Rev. **135**, A1115 (1964).
[25] L. Bryde, N. O. Lassen, and N. O. R. Poulson, Kgl. Danske Videnskab. Selskab, Mat. Fys. Medd. **33**, No. 8 (1962).
[26] J. Lindhard, M. Scharff, and H. E. Schiott, Kgl. Danske Videnskab. Selskab, Mat. Fys. Medd. **33**, No. 14 (1963).
[27] L. Winsberg and J. M. Alexander, Phys. Rev. **121**, 518 (1961).

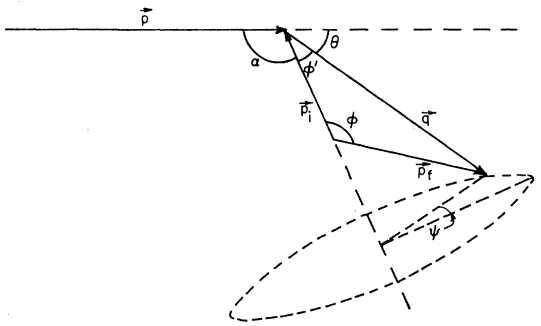

FIG. 2. Kinematics of the $(p,p\pi^+)$ reaction.

IV. CALCULATIONS

Ericson *et al.*[1] have made a rather crude calculation of the excitation function for the $(p,p\pi^+)$ reaction at high energies, using many simplifying assumptions. They used the impulse approximation and made the assumption that the distortion effects, namely absorption of the incident and outgoing waves, were separable and were factored out of the matrix element. Plane waves were thus used in the matrix element, and the absorption, or reduction factor, was evaluated separately. They obtained the following expression for the cross section:

$$\sigma = R\int \frac{d\sigma}{dq^2} \sum_{\substack{n \\ E_n^* \leqslant B}} |F_{no}(q)|^2 dq^2, \qquad (4)$$

where R is the reduction factor, $d\sigma/dq^2$ is the differential cross section for reaction (1), and the last term is the sum of squared mixed-form factors for the initial and final nuclear states, o and n, where the sum is taken over all final states n of the residual nucleus which are stable with respect to particle emission. Ericson *et al.* estimated the sum of the squares of mixed-form factors from a degenerate Fermi gas model of the nucleus, and used OPE theory in the pole approximation[3] to obtain $d\sigma/dq^2$. The reduction factor was estimated under the assumption that the outgoing particles travel as a single entity with the same trajectory and average cross section for collision with the nucleons in the nucleus as the incident proton. The excitation function thus obtained by Ericson *et al.* is in rough agreement with the experimental excitation function except at low energies ($<\sim 1.5$ GeV).[28]

In their evaluation of the nuclear form factors, Ericson *et al.*[1] took into account the effect of Fermi motion on the momentum transfer and also in determining the fractional volume of the nucleus in momentum space which can contribute to the $(p,p\pi^+)$ reaction. However, for the kinematics of the reaction

[28] A calculation of the $(p,p\pi^+)$ excitation function has also been reported by V. S. Barashenkov and V. M. Maltsev, Acta Phys. Polon., Suppl. **22**, 173 (1962). However, these authors did not take into account the effects of the Fermi momentum and the limitation of low excitation energy on the region of integration over the momentum transfer variable.

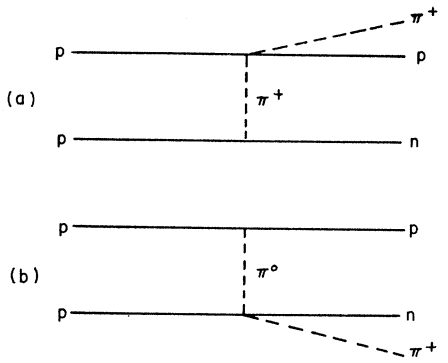

FIG. 3. Diagrams for reaction (1).

they made the implicit approximation that the target proton in the nucleus was stationary. This resulted in the effective threshold in their calculated excitation function being several hundred MeV too high. The main consequence of including the Fermi motion in the reaction kinematics is to change the volume of phase space available to the final state.

The derivation of the expression for the nuclear form factors including the effect of Fermi motion on the kinematics closely follows that of Ericson *et al.*[1] We start with

$$\sigma=R\int\frac{\partial^3\sigma}{\partial^3\mathbf{q}}\sum_{E^*\leqslant B}|F_{fi}(\mathbf{q})|^2d^3\mathbf{q},$$

$$=RZ\int(\tfrac{4}{3}\pi\mathbf{P}_i^3)^{-1}d^3\mathbf{p}_i\frac{\partial^3\sigma}{\partial^3\mathbf{q}}d^3\mathbf{q},$$

where Z is the number of protons in the target nucleus, $\mathbf{P}_i$ is the Fermi momentum of the protons,[29] $\mathbf{p}_i$ is the momentum of the struck proton, and $\partial^3\sigma/\partial^3\mathbf{q}$ has been substituted for $\partial\sigma/\partial q^2$ in Eq. (4) since six variables are needed for a complete description of the kinematics of the target and recoil nucleons. Changing variables to $\mathbf{p}_i$ and $\mathbf{p}_f$ ($\mathbf{p}_f$ is the momentum of the recoil neutron; $\mathbf{p}_f=\mathbf{p}_i+\mathbf{q}$) and writing out the differentials we get

$$\sigma=R\frac{3Z}{4\pi\mathbf{P}_i^3}\int\frac{\partial^3\sigma}{\partial^3\mathbf{q}}p_i^2dp_id\cos\alpha d\beta p_f^2dp_fd\cos\phi d\psi.$$

The various angles and momentum vectors are shown in Fig. 2. We now integrate over the azimuthal angle β and change the variables $\cos\phi$ and ψ to q^2 and w^2 using $2qp_ip_f(\partial^3\sigma/\partial^3\mathbf{q})d\cos\phi d\psi=(\partial^2\sigma/\partial q^2\partial w^2)dq^2dw^2$;

$$\sigma=R\frac{3Z}{4\mathbf{P}_i^3}\int\frac{\partial^2\sigma}{\partial q^2\partial w^2}d\cos\alpha p_idp_ip_fdp_f\frac{1}{q}dq^2dw^2. \quad (5)$$

[29] The boldface **P** and **T** are the Fermi momentum and Fermi energy. The subscripts i and f refer to the *protons* in the *target* nucleus and the *neutrons* in the *product* nucleus, respectively. The Fermi energy of the neutrons in the product nucleus was defined as the Fermi energy of the protons in the target nucleus minus the Q of the reaction ($Q=-2.6$ MeV for the $Cu^{65}(p,p\pi^+)Ni^{65}$ reaction) in order to make the reaction energetics consistent. Also, the potential well was assumed to be zero for the incident and outgoing particles.

The expression for the differential cross section, $\partial^2\sigma/\partial q^2\partial w^2$, for diagram (a) in Fig. 3 which was obtained from OPE theory in the pole approximation[3] is

$$\frac{\partial^2\sigma}{\partial q^2\partial w^2}=\frac{f^2}{2\pi\mu^2F^2}\frac{q^2}{(q^2+\mu^2)^2}R(w)\sigma(w), \quad (6)$$

where the charged pion-nucleon coupling constant $f^2=0.16$, μ is the pion mass, F is the invariant flux and is given by $F=Up_u$; U and p_u are the total energy and momentum in the over-all c.m. system and are given by $U^2=2(1+EE_i-pp_i\cos\alpha)$ and $p_u^2=U^2/4-1$. (The units $m_p=c=1$ are used throughout.) The function $R(w)=\frac{1}{2}[w^4-2(1+\mu^2)w^2+(1-\mu^2)^2]^{1/2}$ and $\sigma(w)$ is the total π^+-p cross section at c.m. energy w. Since the total π^+-p rather than the elastic π^+-p cross section is used, Eq. (6) includes all diagrams like (a) in Fig. 3 with more than one pion coming out of the upper vertex. Equation (6) is really a function of the invariant square of the four momentum transfer Δ^2 rather than the square of the three momentum transfer q^2. The approximation has been made that $q^2=\Delta^2$ while actually $q^2=\Delta^2+\Delta E^2$. This is an excellent approximation for the $(p,p\pi^+)$ reaction because ΔE^2 is always very small compared with q^2. The use of Eq. (6) will be discussed further below. Substituting Eq. (6) into Eq. (5), we now obtain for the $(p,p\pi)$ cross section

$$\sigma=R\frac{3Zf^2}{8\pi\mu^2\mathbf{P}_i^3}\int_{-1}^{+1}d\cos\alpha\int_{p_{i,\min}}^{\mathbf{P}_i}\frac{p_i}{F^2}dp_i\times\int_{\mathbf{P}_f}^{p_{f,\max}}dp_f\int_{p_f-p_i}^{p_f+p_i}\frac{q}{(q^2+\mu^2)^2}dq^2\times\int_{w_{\min}^2}^{w_{\max}^2}R(w)\sigma(w)dw^2. \quad (7)$$

The limits of the integrations are as follows:

$$p_{i,\min}=[(\mathbf{T}_i+1-B)^2-1]^{1/2},$$
$$p_{f,\max}=[(E_i-Q+B)^2-1]^{1/2},$$
$$\mathbf{P}_f=[(\mathbf{T}_i+1-Q)^2-1]^{1/2},$$

where B is the excitation energy at which particle emission predominates over gamma-ray de-excitation, $Q=-Q_\beta-m_e$, and Q_β is the beta-decay energy of the $(p,p\pi^+)$ product nuclide;

$$w_{\min,\max}^2=2pq(\cos\theta)_{\min,\max}+1-q^2-2E\Delta E\geqslant(1+\mu)^2, \quad (8)$$

where

$$(\cos\theta)_{\min,\max}=-\cos(\alpha\mp\phi'),\ \cos\phi'=(q^2+p_i^2-p_f^2)/2p_iq,$$

p and E are the momentum and energy of the incident proton, $\Delta E=E_f-E_i+q^2/2A$, and A is the mass number of the recoil nucleus.

The main difference between Eq. (7) and the expression obtained by Ericson *et al.*[1] is in the limits of the integration over w^2. They used kinematics for a stationary target proton for which the lower limit is always $(1+\mu)^2$, and the upper limit is obtained from Eq. (8) for $w_{\max}^2$ with $(\cos\theta)_{\max}=1$ and $\Delta E=q^2/2$, (nonrelativistically, the kinetic energy of the recoil neutron). The range of the variable w^2 obtained from the limits for Eq. (7) is, on the average, smaller than that gotten from stationary target nucleon kinematics except at low energies ($<\sim 1.5$ GeV) where it is larger. In other words, the volume of phase space available to the nuclear reaction is less for a moving target nucleon than it is for a stationary target nucleon except at low energies.

The forward projection of the kinetic energy of the recoil nucleus is obtained from Eq. (3)

$$T\cos\theta=\frac{q^2}{2A}\,\frac{w^2-1+q^2+2E\Delta E}{2pq},$$

and an expression for the perpendicular projection $T\sin\theta$ is obtained by expressing $\sin\theta$ in terms of $\cos\theta$. The average values of these quantities and also $\langle q^2\rangle_{\rm av}$ and $\langle w^2\rangle_{\rm av}$ were calculated using the complete integrand of Eq. (7) as a weighting function. The integrations were performed numerically on the BNL IBM 7094 computer. The π^+-p total cross sections were taken from published values.[30] For the calculation at 28 GeV, π^+-p cross sections were needed up to $\sim$18 GeV incident pion energy. The parameter B is nominally the separation energy of a neutron from the $(p,p\pi^+)$ product nucleus which is 6.14 MeV for Ni^{65}. (The separation energy of a proton from Ni^{65} is 13.5 MeV.) However, gamma-ray emission can predominate over particle evaporation above the threshold for particle emission.[31] If the spins of the various levels in Ni^{64} and the distribution of spins from the particle-hole excitations in the Ni^{65} product nuclei are taken into account, one finds, as a rough estimate, that de-excitation by gamma-ray emission is on the average more probable than neutron evaporation up to an excitation energy of 8–9 MeV.[32] This introduces an uncertainty into the magnitude of the calculated cross sections since they are very nearly exactly proportional to B^2. A value of 8.5 MeV was used in these calculations. It should be emphasized that this estimate of B is based on the assumption that the $(p,p\pi^+)$ reaction populates only particle-hole states in Ni^{65}.

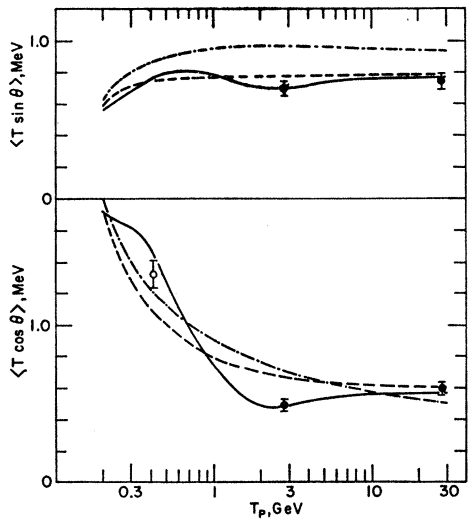

FIG. 4. Average projected recoil energies for the $Cu^{65}(p,p\pi^+)Ni^{65}$ reaction. The experimental points are: ○, Fung and Turkevich (Ref. 6) and ●, this work. The solid curves are the projected recoil energies calculated with OPE theory, the dashed curves are those calculated with OPE theory and a constant π^+-p cross section, and the dot-dashed curves are those calculated from three-body invariant phase space.

The only adjustable parameter in these calculations is the Fermi momentum. The term $\mathbf{P}_i^3$ in the denominator of Eq. (7) comes from a normalization to the number of initially occupied momentum states while the Fermi momentum appearing in the limits of the integrations in Eq. (7) primarily affects the upper limit of the q^2 integration and is thus sensitive to the actual nucleon momentum distribution in the nucleus. For this reason $\mathbf{P}_i$ in the denominator was fixed at 234 MeV/c. This number was obtained with a radius parameter $r_0=1.25$ F. Only the Fermi momentum appearing in the limits of the integration in Eq. (7) was considered an adjustable parameter. Since the poorly known reduction factor has canceled out of the equations for $\langle T\cos\theta\rangle_{\rm av}$ and $\langle T\sin\theta\rangle_{\rm av}$, the recoil data at 2.8 and 28 GeV were used to fix $\mathbf{P}_i$. The calculated average recoil energies $\langle T\cos\theta\rangle_{\rm av}$ and $\langle T\sin\theta\rangle_{\rm av}$ are approximately proportional to $\mathbf{P}_i^2$. The shape of the calculated excitation function, however, is largely independent of $\mathbf{P}_i$.

The results of the calculations are shown in Figs. 1 and 4 as solid lines along with the experimental data. The effective recoil ranges have been converted to energies using the range-energy relationship presented in the previous section. The recoil calculations will be discussed first. The Fermi momentum which gave the best fit to the data was found to be 286 MeV/c which corresponds to a Fermi energy of 42.5 MeV. All of the recoil data agree well with the calculation over a wide range of incident proton energies with this single choice for the Fermi momentum. The point for $\langle T\cos\theta\rangle_{\rm av}$ at

[30] H. P. Noyes and D. N. Edwards, Phys. Rev. **118**, 1409 (1960); T. J. Devlin, B. J. Moyer, and V. Perez-Mendez, *ibid.* **125**, 690 (1962); J. C. Brisson, J. F. Detoeuf, P. Falk-Variant, L. Van Rossum, and G. Valladas, Nuovo Cimento **19**, 210 (1961); M. J. Longo and B. J. Moyer, Phys. Rev. **125**, 701 (1962); A. N. Diddens, E. W. Jenkins, T. F. Kycia, and T. F. Riley, Phys. Rev. Letters **10**, 262 (1963); and S. J. Lindenbaum, W. A. Love, J. A. Niederer, S. Ozaki, J. J. Russell, and L. C. L. Yuan, *ibid.* **7**, 352 (1961).

[31] J. R. Grover, Phys. Rev. **123**, 267 (1961).

[32] Neutron transmission coefficients were taken from E. H. Auerbach and F. E. J. Perey, Brookhaven National Laboratory Report No. BNL-765, 1962 (unpublished).

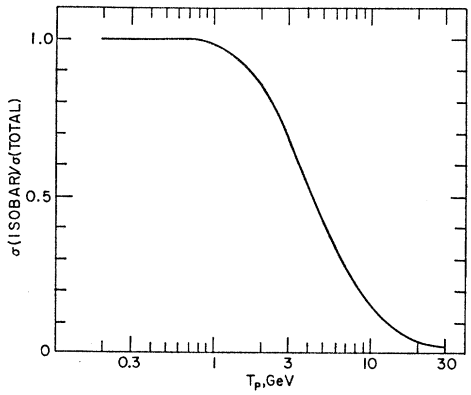

FIG. 5. Fraction of the total calculated $(p,p\pi^+)$ cross section due to the $(\frac{3}{2},\frac{3}{2})$ resonance.

0.41 GeV of Fung and Turkevich[6] deviates from the calculated curve by only 1.4 standard deviations and it should be noted that since those authors did not quote an error estimate for their measurement it was assumed to have the same uncertainty as the measurements of this work.

In order to test the sensitivity of the calculation to the OPE description of reaction (1) a calculation was performed using three-body invariant phase space for reaction (1) for which

$$\frac{\partial^2\sigma}{\partial q^2 \partial w^2} \propto \frac{1}{F^2}\frac{R(w)}{w^2}$$

is substituted into Eq. (5). The results of this calculation are shown in Fig. 4 as the dot-dashed lines. The same Fermi momentum was used in the three-body phase-space calculation as was used in the OPE calculation, but it is clear that no value of the Fermi momentum will give good agreement with all of the data. It would have been better, of course, to have used an incident-energy-dependent average of 3, 4, 5, etc., body-phase space but insufficient information exists for obtaining such an average.

The OPE calculation was also done with a constant pion-proton total cross section in order to investigate the effect of the $(\frac{3}{2},\frac{3}{2})$ resonance on the recoil properties. The results of this calculation are shown in Fig. 4 as the dashed lines. It can be seen that the influence of the resonance is strong, giving rise to the inflections in the solid curves.

A value of 286 MeV/c for the Fermi momentum is larger than that for a zero-temperature Fermi gas of protons confined in a sphere the size of a nucleus. This is probably an indication that the sharp cutoff in the Fermi momentum distribution is unrealistic and that a more reasonable momentum distribution would be one which drops off gradually and extends considerably beyond the Fermi momentum. Another important consideration is that the $(p,p\pi^+)$ reaction is very likely restricted to the surface of the nucleus. Thus the apparent momentum distribution of the struck proton may depend as much on the localization of the reaction sites in the nucleus as it does on the nuclear wave functions in the same way that that localization affects momentum transfer distributions obtained from $(p,2p)$ quasifree scattering experiments.[33]

The calculated excitation function is presented with the experimental cross sections in Fig. 1. The reduction factor R has been assumed to be independent of energy, and the calculated excitation function has been arbitrarily normalized to the experimental point at the maximum, 1.4 GeV. The general features of the experimental excitation function are reproduced by the calculation but there is no detailed agreement between the two. Given the crudeness of the calculation, however, the agreement should be considered satisfactory. The reduction factor obtained from the normalization at 1.4 GeV is 0.157, and decreases to 0.098 at 28 GeV. This is more than adequate agreement with the crude estimate of $\sim$0.1 made by Ericson *et al.*[1]

The calculated excitation function obtained by Ericson *et al.* fits the experimental data above $\sim$1.5 GeV about as well as the present calculation. It was not possible, however, to fit both the forward and perpendicular recoil data at either 2.8 or 28 GeV using the expression for the cross section given by Ericson *et al.* This shows that the use of stationary target nucleon kinematics is not an approximation which becomes valid at high energies.

The excitation function calculated with a constant σ_{π^+-p} is shown in Fig. 1 as the dashed curve (arbitrarily normalized at 30 GeV). This makes it abundantly clear that the peak in the excitation function is due to the $(\frac{3}{2},\frac{3}{2})$ pion-nucleon resonance. The contribution of this resonance to the calculated excitation function was evaluated by performing the calculation with the parameter w restricted to values less than 1.51. The results of this calculation are shown in Fig. 5 as the fraction of the total calculated cross section due to the $(\frac{3}{2},\frac{3}{2})$ resonance as a function of incident proton energy. This broad definition of the resonance, $1.15 \leqslant w \leqslant 1.51$, was chosen (rather arbitrarily) because the experimental π^+-p cross section data can be fit to a Breit-Wigner resonance formula within these limits.[34]

Equation (6) was obtained from OPE theory in the pole approximation,[2] i.e., the corrections ascribed to off-the-mass-shell scattering and pionic form factors were neglected. These corrections have been determined empirically in the region between 1 and 3 GeV but are unknown at higher energies.[4] These corrections, which reduce the cross section as the momentum transfer is increased, become important only near the maximum momentum transfer allowed in the $(p,p\pi^+)$ reaction, while the calculation with the simple OPE theory shows

[33] See, e.g., P. A. Benioff, Phys. Rev. **119**, 324 (1960); K. L. Lim and I. E. McCarthy, *ibid.* **133**, B1006 (1964).

[34] M. Gell-Mann and H. M. Watson, Ann. Rev. Nucl. Sci. **4**, 219 (1954).

that the contribution of these larger momentum transfers to the $(p,p\pi^+)$ reaction is already relatively small. Thus, the use of the more exact OPE theory in this calculation at incident energies less than 3 GeV would not have changed the general nature of the results except to increase slightly the value of the Fermi momentum required to fit the recoil data. Equation (6) begins to lose validity below about 800 MeV because it neglects both final state interactions and the interference term between diagram (a) in Fig. 3 and the diagram resulting from the exchange of the initial protons. Ferrari and Selleri[3] have found that this interference term contributes 10–20% to the total cross section for reaction (1) at incident energies around 1 GeV and it should become more important at lower energies. The contribution of this interference term at the low momentum transfers selected by the $(p,p\pi^+)$ reaction, however, is less than that for the total cross section for reaction (1). At energies less than 500–600 MeV other interference terms also begin to become important.

Reaction (1) also has a contribution from diagram (b) in Fig. 3. This diagram can contribute to the $(p,p\pi^+)$ reaction only in the region of the $(\frac{3}{2},\frac{3}{2})$ resonance, since the pion proton scattering at the lower vertex involves charge exchange, and the charge exchange cross section becomes quite small above the $(\frac{3}{2},\frac{3}{2})$ resonance.[35] The cross section for diagram (b) near the $(\frac{3}{2},\frac{3}{2})$ resonance is only $\frac{1}{9}$ that for diagram (a). The contribution of diagram (b) to the $(p,p\pi^+)$ reaction is further reduced for two reasons. The momentum transfer distribution is not as sharply peaked at low momentum transfers as it is for diagram (a). It is estimated that this would reduce its contribution to the $(p,p\pi^+)$ reaction by a factor of about two. The pion in diagram (b) will usually have a lab kinetic energy in the vicinity of the $(\frac{3}{2},\frac{3}{2})$ resonance while the pion in diagram (a) will in general have a lab kinetic energy greater than the $(\frac{3}{2},\frac{3}{2})$ resonance and often greater than the first two prominent $T=\frac{1}{2}$ resonances. Thus, the pion in diagram (b) will be less likely to leave the nucleus without colliding with a nucleon than the pion in diagram (a). The probability of escape of the pion in diagram (a) will be further enhanced in the region of the $(\frac{3}{2},\frac{3}{2})$ resonance by the finite lifetime of the $(\frac{3}{2},\frac{3}{2})$ isobar. The mean free path with respect to decay of the isobar, given by $\lambda=\tau\beta\gamma c$, is 2.6 F for an isobar produced at 1 GeV incident energy and 6.0 F for an isobar produced at 2.8 GeV. Thus, if the nucleon-isobar cross sections are not much different from nucleon-nucleon cross sections, the isobar has a significant probability of leaving the nucleus before it decays. The isobar in diagram (b) has little kinetic energy and will rarely leave the nucleus before decaying. For these reasons it is felt that the contribution of diagram (b) to the $(p,p\pi^+)$ reaction is less than about 2% and can safely be neglected. Likewise, diagrams where pions are produced at both vertices, the so-called double isobar diagrams, have been assumed to make negligible contributions to the $(p,p\pi^+)$ reaction since charge exchange is again required at the lower vertex. Thus the $(p,p\pi^+)$ reaction takes place only through diagram (a) with one or more pions at the upper vertex, and therefore involves pion-proton scattering with isotopic spin $\frac{3}{2}$ only.

[35] V. S. Barashenkov and V. M. Maltsev, Fortschr. Physik **9**, 549 (1961).

V. CONCLUSIONS

The relatively good agreement between the experimental data for the $Cu^{65}(p,p\pi^+)Ni^{65}$ reaction and the simple theoretical treatment of Ericson *et al.*[1] indicates that their description of the reaction is basically valid. The dominance of the $(\frac{3}{2},\frac{3}{2})$ pion-nucleon resonance in the $(p,p\pi^+)$ reaction at incident energies below 3 GeV demonstrates that the $(p,p\pi^+)$ reaction is indeed sensitive to the details of the elementary-particle reaction (1). That the agreement between the experimental data and the calculations extends to 28 GeV could be considered coincidental in view of the fact that the simple OPE theory for reaction (1) is untested at very high energies. However, if reaction (1) takes place through the exchange of a particle substantially heavier than a pion, such as a rho, or through some process other than particle exchange, the momentum transfer distribution for reaction (1) would probably be less peaked at low-momentum transfers, and the recoil energies at 28 GeV would tend to be more like those calculated from three-body phase space. Thus these experiments suggest that the simple OPE theory for reaction (1) is as valid at 28 GeV as it is at 1–3 GeV.

The $(p,p\pi^+)$ reaction requires the exchange of one unit of isotopic spin since the pion-proton interaction at the upper vertex in diagram (a) can have isotopic spin $\frac{3}{2}$ only. Even if there is a substantial contribution to the $(p,p\pi^+)$ reaction at 28 GeV from diagrams with pions coming out at both vertices, the exchange of one unit of isotopic spin is still required since charge exchange must take place at the lower vertex and pion-proton charge exchange occurs mostly with isotopic spin $\frac{3}{2}$.[35] The inelastic proton-proton scattering data reported by Cocconi *et al.*[36] show that production of the $(\frac{3}{2},\frac{3}{2})$ resonance decreases rapidly with increasing energy and momentum transfer while the isotopic spin $\frac{1}{2}$ resonances remain quite prominent. In fact the $(\frac{3}{2},\frac{3}{2})$ resonance was not seen at all above $\sim$8 GeV. It was suggested that this difference in the production of the isotopic spin $\frac{3}{2}$ and $\frac{1}{2}$ states is associated with the exchange of isotopic spin 1 and 0, respectively. The cross section obtained for the $(p,p\pi^+)$ reaction at 28 GeV indicates that the exchange of one unit of isotopic spin is not greatly suppressed at very high energies, although the present data do not necessarily imply that the $(\frac{3}{2},\frac{3}{2})$ resonance is produced at these energies. It should be noted that at the energies where the $(\frac{3}{2},\frac{3}{2})$ resonance

[36] G. Cocconi, E. Lillethun, J. P. Scanlon, C. A. Stahlbrandt, C. C. Ting, J. Walters, and A. M. Wetherell, Phys. Letters **8**, 134 (1964).

was not observed in the inelastic proton-proton scattering experiments the momentum transfers were larger than those included in the $(p,p\pi^+)$ reaction.

ACKNOWLEDGMENTS

The constant encouragement of Dr. G. Friedlander and the valuable discussions with and suggestions from Professor J. M. Alexander, Dr. J. B. Cumming, Dr. T. Ericson, Dr. J. R. Grover, Professor S. Kaufman, Dr. R. F. Peierls, Dr. R. Sternheimer, Professor N. Sugarman, Professor A. Turkevich, and Professor L. Winsberg are greateully acknowledged. The author is particularly indebted to Dr. A. M. Poskanzer whose suggestions and generous assistance were indispensable and are deeply appreciated. Thanks are also due to Dr. R. W. Stoenner and his group for performing the chemical yield analyses and to the operating staffs of the Cosmotron and AGS.

PHYSICAL REVIEW VOLUME 138, NUMBER 3B 10 MAY 1965

Intermediate-State Theory of Single-Particle Resonances*

L. GARSIDE AND W. M. MACDONALD
Department of Physics and Astronomy, University of Maryland, College Park, Maryland
(Received 21 December 1964)

The $d_{3/2}$ state in oxygen is observed as a very sharp scattering resonance in $O^{16}(n,n)$ O^{16}. The state is a "virtual" state, therefore, and its inclusion among the single-particle discrete states employed in the shell-model description of states of O^{16} requires some justification. In this paper a unified reaction theory recently given by one of the authors is used as the basis of a description in which the resonance is described as arising from the virtual transitions into a true bound state. The continuum states of this description are nonresonant because the continuum $d_{3/2}$ resonance is replaced by a bound $d_{3/2}$ state which plays the role of a new "doorway state." This description leads to the conventional shell-model description of the particle-hole resonances of O^{16} and simplifies the description of the interaction between virtual and bound states.

I. INTRODUCTION

THE relationship between the single-particle resonance of a shell-model potential and resonances associated with particle-hole states is extremely crucial to a consistent, indeed a correct, calculation of a nuclear-reaction cross section. In fact, a considerable amount of insight into the correctness or the usefulness of a particular formulation of reaction theory can be gained from the way in which single-particle resonances are handled, particularly when they occur near thresholds. A resonance associated with any nonzero value of angular momentum becomes increasingly narrow if the resonance energy is decreased. Not only does the resonance then become more difficult to distinguish experimentally from a "compound nuclear resonance," but appreciable configuration mixing with discrete shell-model states may make this distinction less meaningful. The single-particle resonance is parceled out among more complex levels (e.g., two-particles, one-hole states) in precisely the manner discussed by Lane, Thomas, and Wigner.[1] We shall learn from our analysis of a low-lying resonance that in this situation the "doorway state" is a single-particle state, or one quasiparticle state.

The considerations of this paper are based on the shell-model reaction theory outlined in earlier papers,[2] and the results of a specific calculation will be presented for the $d_{3/2}$ resonance in the elastic scattering of neutrons on O^{16}. For the purpose of testing a reaction theory the situation which obtains in the nuclei with $A=15$, 16, and 17 is nearly ideal and this paper is preliminary to a more extensive survey of the reactions involving these nuclei.

The $d_{3/2}$ resonance observed in $O^{16}(n,n)O^{16}$ occurs at 0.934 MeV with a width of only 90 keV. This width is approximately what one should expect for a d-wave resonance produced by the average Hartree field in this nucleus. A corresponding resonance also occurs in proton scattering on O^{16}. Since these resonances arise from the average potential generated by O^{16}, we should also expect to find $d_{3/2}$ resonances in the nucleon scattering on O^{15} and N^{15}. In the simplest shell model these nuclei are described as belonging to the configuration $1p_{1/2}^{-1}$, a hole in the $1p_{1/2}$ shell. Overlooking the distinction between bound and continuum states for the moment, we could describe the resonance observed in nucleon scattering on N^{15} and O^{15} as "belonging to the configuration $p_{1/2}^{-1}$ $d_{3/2}$." Similarly if elastic scattering could be performed on O^{15} and N^{15} in their first excited state

* Research supported in part by NASA Contract No. NsG 642 and AEC Contract AT-(40-1)-2098.

[1] A. M. Lane, R. G. Thomas, and E. P. Wigner, Phys. Rev. **98**, 693 (1955).

[2] W. M. MacDonald, Nucl. Phys. **54**, 393 (1964); **56**, 636, 647 (1964).